Journal of Power Sources 195 (2010) 7250–7254

Contents lists available at ScienceDirect

Journal of Power Sources

journal homepage: www.elsevier.com/locate/jpowsour

Short communication

Electrochemical reduction of CO_2 in solid oxide electrolysis cells

Zhongliang Zhan*, Lin Zhao

CAS Key Laboratory of Materials for Energy Conversion, Shanghai Institute of Ceramics, Chinese Academy of Sciences, 1295 Ding-Xi Road, Shanghai 200050, PR China

ARTICLE INFO

Article history:
Received 13 April 2010
Received in revised form 24 May 2010
Accepted 24 May 2010
Available online 27 May 2010

Keywords:
Solid oxide electrolysis cells
Solid oxide fuel cells
Electrochemical reduction
Carbon dioxide

ABSTRACT

This paper describes results on the electrochemical reduction of carbon dioxide using the same device as the typical planar nickel–YSZ cermet electrode supported solid oxide fuel cells (H_2–CO_2, Ni–YSZ|YSZ|LSCF–GDC, LSCF, air). Operation in both the fuel cell and the electrolysis mode indicates that the electrodes could work reversibly for the charge transfer processes. An electrolysis current density of ≈1 A cm^{-2} is observed at 800 °C and 1.3 V for an inlet mixtures of 25% H_2–75% CO_2. Mass spectra measurement suggests that the nickel–YSZ cermet electrode is highly effective for reduction of CO_2 to CO. Analysis of the gas transport in the porous electrode and the adsorption/desorption process over the nickel surface indicates that the cathodic reactions are probably dominated by the reduction of steam to hydrogen, whereas carbon monoxide is mainly produced via the reverse water gas shift reaction.

1. Introduction

Recently there has been growing interest in operating the solid oxide fuel cell (SOFC) device in a reverse mode, usually involving reduction of water in the negative electrode for a hydrogen–steam gas mixture and evolution of oxygen into air in the positive electrode [1–5]. Such a high temperature electrolysis device has been commonly recognized as a solid oxide electrolysis cell (SOEC). A typical SOEC uses the same set of materials as the SOFC, consisting of yttrium-stabilized zirconia (YSZ) electrolytes, Ni–YSZ fuel electrodes and LSM–YSZ (LSM = lanthanum strontium manganite) air electrodes. Using the state-of-the-art nickel–YSZ cermet electrode configurations, an electrolysis current density as high as 3.6 A cm^{-2} was obtained at 950 °C and 1.48 V with a steam utilization of 37% for an inlet gas mixture of 70% H_2O + 30% H_2% [4]. The mixed conducting oxide of samaria-doped ceria with highly dispersed nanometer-sized Ni catalysts could be used as the SOEC cathode to improve the steam reduction reactions [2]. Ceramic oxide composites such as lanthanum-substituted strontium titanate/ceria were also found to exhibit higher activity than the commonly used Ni–YSZ for the electrolysis of steam [5]. These increasing research and development efforts toward the high temperature SOECs mainly originates from their promising potential of providing a highly efficient production of high purity hydrogen with much less demand for electricity due to the thermodynamically and kinetically favorable operating conditions in comparison with the low temperature alkaline or proton exchange membrane (PEM) electrolysis technologies. Thermodynamic analysis has indicated that the high temperature steam electrolysis system coupled with the high temperature gas cooled reactor could accomplish an overall efficiency of 53% at 800 °C, remarkably higher than 27% for the conventional alkaline water electrolysis [6,7].

The oxygen ionic conductive electrolytes in SOECs enable the electrolysis of carbon dioxide to carbon monoxide as well. However, there are very few reports on the use of the current state-of-the-art nickel–YSZ anode supported SOFCs for the electrochemical reduction of carbon dioxide to carbon monoxide. Sridhar and Vaniman reported on the use of SOECs with platinum electrodes for oxygen production via the electrochemical reduction of CO_2, which may find direct applications in ongoing space missions and in the future human exploration of Mars [8–10]. More importantly, high temperature electrochemical reduction of CO_2 might be a promising alternative to the current technological approaches for fixation of carbon dioxide and conversion to valuable substances. Note that the resulting CO, in combination with hydrogen, can be catalytically converted via Fischer Tropsch or methanation reactions to hydrocarbon fuels [11–13], which can subsequently be consumed by the same device operated in the fuel cell mode to produce electricity as well as steam and carbon dioxide. Since the renewable energy sources such as wind, solar and hydropower could be used to drive the electrolysis process, the widespread implementation of the reversible SOFCs/SOECs promise a carbon-neutral and zero-emission synthetic hydrocarbon economy.

In this paper, electrolysis of carbon dioxide was carried out using the standard planar Ni–YSZ electrode-supported SOFCs operated with 25% H_2–75% CO_2. The results indicated that the commonly used Ni–YSZ electrodes were highly effective for the electrochem-

* Corresponding author. Tel.: +86 21 6998 7669; fax: +86 21 6998 7669.
E-mail address: zzhan@mail.sic.ac.cn (Z. Zhan).

0378-7753/$ – see front matter © 2010 Elsevier B.V. All rights reserved.
doi:10.1016/j.jpowsour.2010.05.037

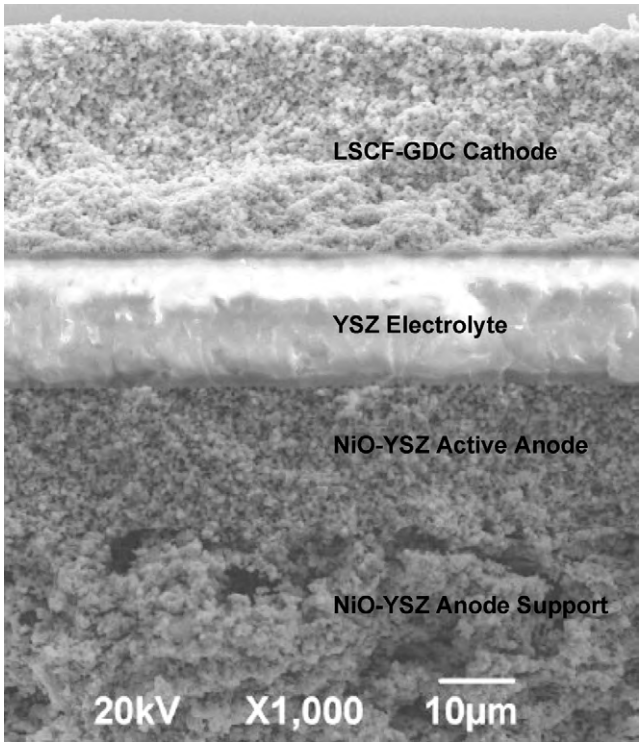

Fig. 1. Fracture cross-sectional SEM micrograph of a typical nickel–YSZ cermet electrode SOEC, Ni–YSZ|YSZ|LSCF–GDC, LSCF.

ical reduction of CO_2 to CO. The possible mechanism of CO_2 reduction was briefly discussed.

2. Experimental

The SOECs used in this study were similar to the current state-of-the-art solid oxide fuel cells being developed world-wide, consisting of Ni–YSZ negative electrode supports, thin YSZ electrolytes, and LSCF–GDC positive electrode (GDC = $Ce_{0.9}Gd_{0.1}O_{1.95}$ and LSCF = $La_{0.6}Sr_{0.4}Co_{0.2}Fe_{0.8}O_3$). The negative electrode substrates were fabricated using the tape casting and tape lamination techniques. Powders of NiO (Fuel Cell Materials), YSZ (TZ-8YS, 7 $m^2\ g^{-1}$, Tosoh) and rice starch were ball-milled in a weight ratio of 40:40:20 for 24 h with appropriate amounts of dispersant, binder, plasticizer and solvent. The resulting homogeneous slurry was then cast under the doctor blade. After drying, green NiO–YSZ sheets of ≈150 μm thick were obtained. Similarly, green sheets of active NiO–YSZ electrodes or YSZ electrolytes (≈20 μm thick) were prepared by casting NiO–YSZ or YSZ slurry that was formed in the same way as in the case of NiO–YSZ substrates except that no pore former was added. Four sheets of NiO–YSZ substrates, one sheet of active NiO–YSZ electrode and one sheet of YSZ electrolyte were then stacked and laminated at 70 °C for 10 min under a pressure of 21 MPa, which were then co-sintered at 1300–1400 °C for 4 h in order to densify the electrolyte layer. LSCF–GDC electrodes were prepared by mixing LSCF powder with GDC powder in a weight ratio of 70:30. A screen printing vehicle (Electro-Science Laboratory) was added to the mixed powder to make a slurry. The slurry was applied onto the YSZ electrolyte coating and fired at 900 °C for 4 h, as previously used to avoid the chemical reaction between LSCF and YSZ [14]. Then a second layer of pure LSCF slurry was applied and fired at 900 °C for 4 h. Fig. 1 shows a representative cross-sectional SEM image of the nickel–YSZ cermet electrode supported SOECs. The electrolyte layer was fully dense and had a thickness of ~15 μm. The positive electrode was ~30 μm thick. Estimated porosities for

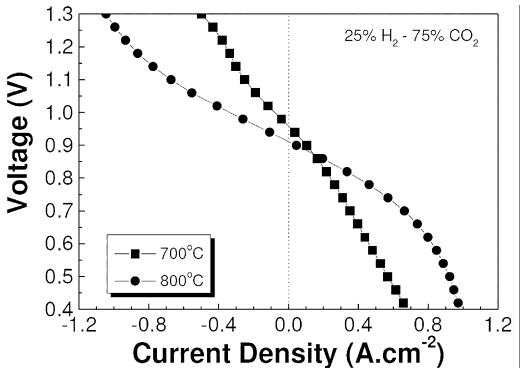

Fig. 2. Voltage versus current density results at various temperatures for a typical Ni–YSZ|YSZ|LSCF–GDC, LSCF, SOEC operated with a 25% H_2–75% CO_2 gas mixture at 200 sccm in the negative electrode and ambient air in the positive electrode.

the negative and positive electrodes were ≈40% and ≈30%, respectively. The cathode area, which defined the cell active area, was 1–2.4 cm^2.

The SOECs were tested in a tube furnace at temperatures from 700 °C to 800 °C, using a standard testing geometry as previously reported [15]. At the beginning of each test, the Ni-based cermet electrode was fully reduced in humidified H_2 at 800 °C. These cells were then tested with H_2–CO_2 fuel mixtures at the negative electrode, while ambient air was maintained in the positive electrode. *I–V* curves and electrochemical impedance spectra (EIS) were obtained using an IM6 Electrochemical Workstation (ZAHNER, Germany). The frequency range for the impedance measurement was 0.1–100 kHz. The effluent from the nickel electrode was sampled using a capillary tube with inlet placed near the negative electrode as previously reported [15], and was analyzed using a quadrupole mass spectrometer after steam was removed from the products with a desiccant. In order to obtain the actual exhaust compositions via quantitative analysis of these spectra, the mass spectrometer system was calibrated using a gas mixture of 25% H_2–75% CO_2 at room temperature. Note that the cracking pattern of gaseous CO overlaps with that of CO_2 at *m*/e = 28. Nevertheless, the contribution to the peak at *m*/e = 28 from gaseous CO could be obtained by subtracting that due to CO_2 cracking, which is always a fraction of the peak at *m*/e = 44. Thus, H_2, CO, and CO_2 were measured directly by mass spectrometer, while steam contents were calculated from mass conservation.

3. Results and discussion

As a baseline, these SOEC devices were first tested in the fuel cell mode with pure hydrogen in the nickel electrode. The power density at 800 °C and 0.7 V was ≈1.2 W cm^{-2}, similar to those reported previously for SOFC operation [16]. Fig. 2 shows the typical voltage *V* versus current density *J* curves for these SOECs operated on 25% H_2–75% CO_2 fuel mixtures at 200 sccm in both the fuel cell and the electrolysis modes at 700 °C and 800 °C. The open circuit voltage (OCV) values ranged from 0.96 V at 700 °C to 0.91 V at 800 °C, slightly higher than the values from 0.94 V to 0.89 V predicted using the effective oxygen partial pressure of the equilibrated fuel. *J* values at a given *V* generally increased with increasing temperature, as typically observed for SOECs [1,4,5]. For example, at a voltage of 1.3 V, the electrolysis current densities increased from 0.5 A cm^{-2} at 700 °C to 1.05 A cm^{-2} at 800 °C. The *J–V* dependence was generally linear near open circuits, *i.e.*, the slope of the *J–V* curve does not change when transitioning from one mode to the other, as previously observed for steam electrolysis [17]. This suggests that the electrodes could work reversibly for the charge transfer reactions. Linear regression analysis of the *V–J* curves yielded the cell inter-

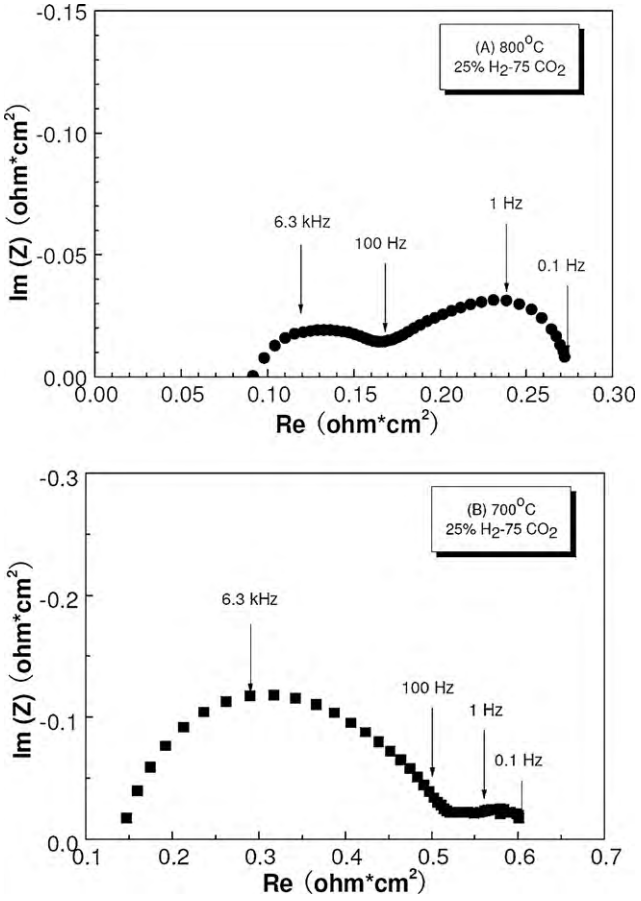

Fig. 3. Nyquist plot of the electrochemical impedance spectroscopy results at open circuit at (a) 800 °C and (b) 700 °C from a typical Ni–YSZ|YSZ|LSCF–GDC, LSCF, SOEC operated with a 25% H_2–75% CO_2 gas mixture at 200 sccm in the negative electrode and ambient air in the positive electrode.

nal area specific resistance (ASR) values near the open circuits, *e.g.*, 0.26 Ω cm^2 at 800 °C and 0.54 Ω cm^2 at 700 °C. Note that there are some discrepancies in the published reports on the reversibility of the same set of materials working in the SOFC and SOEC modes. For example, higher ASR values were observed in the electrolysis mode than in the fuel cell mode for Ni–YSZ|YSZ|LSM–YSZ by Jensen et al. [4] and for Ni–YSZ|YSZ|SDC|LSCF (SDC = samarium doped ceria) by Marina et al. [5], respectively. One possible explanation for these discrepancies is the use of different SOEC anode materials or structures. Pronounced enhancement in the oxygen reduction rate has been observed for LSM under the cathodic dc polarization, a phenomenon termed as current-conditioning or electrode activation [18]. The anodically polarized LSM electrode might be able to explain increased ASR values for Ni–YSZ|YSZ|LSM–YSZ operated in the electrolysis mode while the LSCF electrodes exhibited an constant ASR value in both the fuel cell and the electrolysis modes [19]. The higher ASR values for Ni–YSZ|YSZ|SDC|LSCF in SOECs than in SOFCs could be caused by the presence of the porous SDC interlayer between the electrolyte and the LSCF electrode, which may undergo a reduction reaction of Ce^{4+} to Ce^{3+}.

Fig. 3 shows typical electrochemical impedance spectra at open circuits from these SOECs at (a) 800 °C and (b) 700 °C. The total cell resistance was 0.27 Ω cm^2 at 800 °C and 0.60 Ω cm^2 at 700 °C, in good agreement with the values obtained from the *V–J* curves in Fig. 2. At 800 °C, the Nyquist plot consisted of a small higher frequency depressed arc and a large lower frequency arc. With decreasing temperature, a pronounced increase in the higher frequency depressed arc was observed, whereas the lower frequency

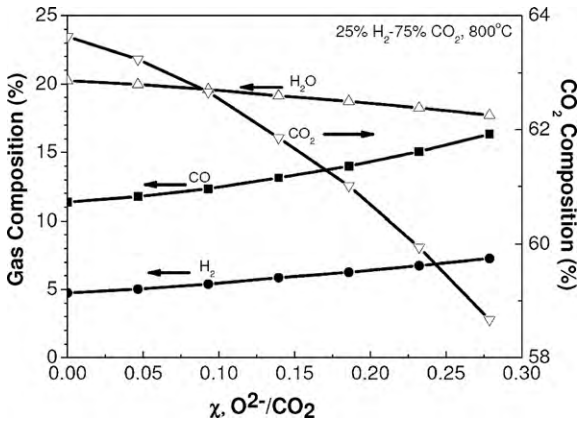

Fig. 4. The product gas composition versus O^{2-}/CO_2 ratio measured during the electrolysis test.

arc only changed slightly as shown for example at 700 °C in Fig. 3 (b). The very weak temperature dependence of the low frequency arc suggests that it might be associated with a gas diffusion process. On the other hand, the high frequency arc followed an Arrhenius dependence, which indicated that it might correspond to a combination of the negative and positive electrode polarization. The overall charge transfer resistance (R^t_{ct}) values are 0.07 Ω cm^2 at 800 °C and 0.38 Ω cm^2 at 700 °C. Note that LSCF has high catalytic activity for oxygen reduction reactions due to its rapid oxygen surface exchange rate and bulk oxygen diffusion rate. Previous electrochemical impedance measurements have shown that the polarization resistance R^p_{ct} values for LSCF–GDC electrodes on YSZ electrolytes could be as low as 0.01 Ω cm^2 at 750 °C and 0.03 Ω cm^2 at 700 °C [20]. These results suggest that the high frequency arc is predominantly associated with the Ni–YSZ negative electrode polarization process, *i.e.*, $R^n_{ct} \approx R^t_{ct}$. Linear fitting of the curve of $\mathrm{Ln}(R^n_{ct})$ versus $1/T$ gives an activation energy value of 1.5 eV for the charge transfer reaction occurring in the negative electrode, close to the value previously observed for the hydrogen oxidation process [21].

The electrolysis products at 800 °C were monitored using an online mass spectrometer. Quantitative analysis of these spectra was performed to obtain the exhaust compositions, as summarized in Fig. 4. At open circuits, the exhaust consisted of 64% CO_2, 20% H_2O, 11% CO and 4.8% H_2. With increasing electrolysis current or O^{2-}/CO_2 ratio, both the CO and H_2 contents increased while the CO_2 and H_2O contents dropped. These results demonstrate that these SOECs are effective for the electrochemical reduction of carbon dioxide to carbon monoxide. At 800 °C, the standard Gibbs free energy for the water gas shift reaction (WGSR) is −400 J mol^{-1}.

$$H_2O + CO \Leftrightarrow H_2 + CO_2 \quad (1)$$

Nonetheless, WGSR has very high reaction rate constants and is thus equilibrium-limited, especially under the catalysis of the Ni–YSZ electrode. Thermodynamic calculations, based upon the chemical reaction (1), show that the percentages of H_2, H_2O, CO and CO_2 for an inlet mixture of 25% H_2–75% CO_2 at open circuits and 800 °C are 6.4, 18.6, 18.6 and 56.4, respectively. As previously estimated [15], comparison of the experimentally measured exhaust compositions with the equilibrium predictions at open circuits yielded a CO_2 utilization of ≈60%, indicative of a flow geometry limitation in the SOEC test. Note that improved gas flow across the surface of the nickel electrode could substantially increase the gas utilization up to 90%, thus giving a better consistency with the thermodynamic prediction [15].

The above results have shown that the state-of-the-art nickel–YSZ cermet electrode supported SOFCs are highly effective

for the electrochemical reduction of carbon dioxide. The overall electrochemical reaction in the negative electrode could be formulated as

$$CO_2\ (g) + V_{\ddot{O}} + 2e' \Rightarrow CO\,(g) + O_O^{\times} \quad (2)$$

where e' represents free electrons from the electrode, $O_O^{\times}$ and $V_{\ddot{O}}$, in Kröger–Vink notation, denote oxygen ions and doubly positive charged oxygen vacancies in the YSZ lattice, respectively. Thermodynamic calculations indicate that there is substantial amount of steam present in the system together with the major component of CO_2. Thus, the CO_2 reduction process in the multiple-component heterogeneous system is very complicated and might proceed in multiple consecutive or parallel steps, including the transport of CO_2/H_2O gas species through the porous nickel electrode, the adsorption of CO_2/H_2O onto the nickel surface, dissociation of CO_2/H_2O molecules, oxygen reduction as well as the desorption of the resulting CO/H_2 from the nickel surface. It is possible that the SOECs simultaneously reduced CO_2 and H_2O. Alternatively, the SOEC cathodic reaction was dominated by reduction of one species. For example, if H_2O were preferentially reduced by the SOECs, the CO product could still be produced via the reverse WGSR with the Ni–YSZ electrode acting as a catalyst. Below a simple analysis of the concentration polarization based on the transport of gaseous species through the porous Ni–YSZ cermet electrode is conducted to provide some insights on the CO_2 electrolysis mechanism.

For the SOECs operating on H_2–CO_2 inlet gas mixtures, H_2, H_2O, CO and CO_2 are present in the gas phase at high temperatures due to the kinetically rapid water gas shift reaction. These gaseous species are transported in the porous Ni–YSZ cermet electrode via molecular diffusion and permeation, and then undergo adsorption and desorption over the nickel surface. Theoretical analysis of concentration polarization by Kim et al. indicates that the limiting current density is correlated with the gas partial pressure, diffusion coefficient as well as the structural factors of the porous electrode [22]. For the anode supported SOFCs, the limiting current density can be given as:

$$J_{al}^{SOFC} = \frac{2FP_{H_2}\varphi D_{H_2}}{RTl_a} \quad (3)$$

where φ is the ratio of porosity to tortuosity, P_{H_2} is the partial pressure of hydrogen in the fuel, D_{H_2} is the diffusion coefficient of hydrogen, l_a is the thickness of the anode (~0.6 mm), and R, T, and F have their usual meaning. As reported previously, the binary diffusion coefficients can be calculated based upon the Stefan–Maxwell equation in multi-component gas mixtures [14]. The calculated diffusion coefficients at 800 °C are 4.86 $cm^2\,s^{-1}$, 1.95 $cm^2\,s^{-1}$, 1.29 $cm^2\,s^{-1}$ and 1.19 $cm^2\,s^{-1}$ for H_2, H_2O, CO and CO_2, respectively. Assume that the SOFC anodic oxidation reactions are dominated by gaseous hydrogen and that CO is converted to CO_2 mainly by the water gas shift reaction, the structure factor (φ) can be calculated from the limiting current value of 1 A cm^{-2} in Fig. 2, yielding $\varphi = 0.022$.

For SOECs, the limiting current could be similarly calculated as

$$J_{al}^{SOEC} = \frac{2F\phi P_i D_i}{RTl_a} \quad (4)$$

where P_i is the partial pressure of steam or carbon dioxide in the gas mixtures, D_i is the diffusion coefficient of steam or carbon dioxide. The calculated limiting current densities are 1.2 A cm^{-2}, 0.7 A cm^{-2} and 0.8A cm^{-2} for steam dominated cathodic reduction, CO_2 dominated cathodic reduction and simultaneous cathodic reductions of steam and CO_2, respectively. Comparison of these values with the experimentally observed ≈1.1 A cm^{-2} as shown in Fig. 2 suggests that the electrolysis reactions over the porous nickel–YSZ cermet electrode are predominated by the reduction of steam to hydrogen. The resulting decrease in steam and increase in hydrogen in the gas mixtures promote the reversed water gas shift reaction, thus consuming CO_2 and producing CO.

Considering the adsorption/desorption of steam and carbon dioxide on the nickel electrode as shown in Eqs. (5) and (6)

$$H_2O\ (g) + Ni\,(s) \underset{K_{-1}}{\overset{K_1}{\longleftrightarrow}} H_2O\,(s) \quad (5)$$

$$CO_2\,(g) + Ni(s) \underset{K_{-2}}{\overset{K_2}{\longleftrightarrow}} CO_2\ (s) \quad (6)$$

The surface adsorption rate constant K is defined as

$$K_i = \frac{P_i}{N_A\Gamma\sqrt{2\pi M_i k_B T}} S_i^0 \quad (7)$$

where S_i^0 is the initial sticking coefficient, M_i the molecular mass of the gas species, P_i the partial pressure, N_A Avogadro's number, k_B the Boltzmann constant and Γ the number of free adsorption sites on the nickel surface (2.6×10^{-9} mol cm^{-2}) [23]. The desorption rate constants K_{-1} and K_{-2} follow the Arrehenius equation [23]. Using the data from reference [23] and the equilibrium gas composition, the adsorption and desorption rate constants can be calculated as follows: $K_1 = 2.3 \times 10^6\ s^{-1}$, $K_2 = 4.4 \times 10^2\ s^{-1}$, $K_{-1} = 4.1 \times 10^9\ s^{-1}$ and $K_{-2} = 3.7 \times 10^6\ s^{-1}$. Since the overall cathodic reduction rate is generally limited by the charge transfer reaction, it is thus reasonable to assume that the adsorption–desorption process is kinetically rapid enough to reach equilibrium. Accordingly, the ratio of nickel surface coverage of steam to carbon dioxide could be calculated as $\theta_{H_2O}/\theta_{CO_2} = K_1K_{-2}K_{-1}K_2 = 4.7$, which indicates that H_2O is much more preferably adsorbed onto the nickel surface than CO_2, even though the latter has a higher content in the fuel mixture (56% of CO_2 versus 18% of H_2O in equilibrium at 800 °C). The superior adsorption capability of steam further supported the above conclusion that the electrolysis reaction over the Ni–YSZ cermet electrode is dominated by the reduction of steam to hydrogen.

4. Conclusions

We have demonstrated that the current state-of-the-art nickel–YSZ cermet electrode supported electrolytic cells could work reversibly in either fuel cell or electrolysis mode. The results from mass spectra showed that the nickel–YSZ cermet electrode is catalytically active for the electrochemical reduction of CO_2 to CO. For an inlet gas mixture of 25% H_2–75% CO_2, an electrolysis current density of 1 A cm^{-2} could be achieved at 800 °C and 1.3 V. Gas transport and adsorption/desorption analysis suggested that reduction of steam to hydrogen predominates the cathodic reactions, whereas carbon monoxide is mainly yielded via the reverse water gas shift reaction with rapid kinetics at elevated temperatures.

Acknowledgement

The authors gratefully acknowledge the financial support of Science and Technology Commission of Shanghai Municipality under the project 09JC1415200.

References

[1] K. Eguchi, T. Hatagishi, H. Arai, Solid State Ionics 86–88 (1996) 1245–1249.
[2] H. Uchida, N. Osada, M. Watanabe, Electrochem. Solid State Lett. 7 (12) (2004) A500–A502.
[3] A. Hauch, S.H. Jensen, S. Ramousse, M. Mogensen, J. Electrochem. Soc. 153 (2006) A1741–A1747.
[4] S.H. Jensen, P.H. Larsen, M. Mogensen, Int. J. Hydrogen Energy 32 (2007) 3253–3257.
[5] O.A. Marina, L.R. Pederson, M.C. Williams, et al., J. Electrochem. Soc. 154 (5) (2007) B452–B459.
[6] M. Liu, B. Yu, J. Xu, J. Cheng, J. Power Sources 177 (2008) 493–499.

[7] S. Fujiwara, S. Kasai, H. Yamauchi, et al., Prog. Nucl. Energy 50 (2008) 422–426.
[8] K.R. Sridhar, B.T. Vaniman, Solid State Ionics 93 (1997) 321–328.
[9] G. Tao, K.R. Sridhar, C.L. Chan, Solid State Ionics 175 (2004) 615–619.
[10] G. Tao, K.R. Sridhar, C.L. Chan, Solid State Ionics 175 (2004) 621–624.
[11] J.H. Lunsford, Catal. Today 63 (2000) 165–174.
[12] J.R. Rostrup-Nielsen, Catal. Today 71 (2002) 243–247.
[13] D.J. Wilhelm, D.R. Simbeck, A.D. Karp, R.L. Dickenson, Fuel Process. Technol. 71 (2001) 139–148.
[14] Z. Zhan, S. Barnett, Solid State Ionics 176 (2005) 871–879.
[15] Z. Zhan, Y. Lin, M. Pillai, I. Kim, S. Barnett, J. Power Sources 161 (1) (2006) 460–465.
[16] Y. Lin, Z. Zhan, J. Liu, S. Barnett, Solid State Ionics 176 (23–24) (2005) 1827–1835.
[17] S. Elangovan, J.J. Hartvigsen, L.J. Frost, Int. J. Appl. Ceram. Technol. 4 (2) (2007) 109–118.
[18] B. Yildiz, K.C. Chang, D. Myers, J.D. Carter, H. You, Proceedings of the Lucerne Fuel Cell Forum 2006 7th European Solid Oxide Fuel Cell Forum, 3–7 July, 2006.
[19] W.S. Wang, Y.Y. Huang, S.W. Jung, J.M. Vohs, R.J. Gorte, J. Electrochem. Soc. 153 (11) (2006) A2066–A2070.
[20] E. Perry Murray, M.J. Sever, S.A. Barnett, Solid State Ionics 148 (1–2) (2002) 27–34.
[21] Baukje de Boer, SOFC anodes: hydrogen oxidation at porous nickel and nickel/yttria-stabilised zirconia cermet electrodes, Thesis, University of Twente, 1998.
[22] J.W. Kim, A.V. Virkar, K.Z. Fung, K. Mehta, S.C. Singhal, J. Electrochem. Soc. 146 (1) (1999) 69–78.
[23] E.S. Hecht, G.K. Gupta, H. Zhu, et al., Appl. Catal. A: Gen. 295 (2005) 40–51.